2011

Reliability, Flexibility, and Environmental Impact of Alternative Arterial Offset Optimization Objective Functions

Christopher M. Day
Purdue University, cmday@purdue.edu

Thomas M. Brennan Jr
Purdue University

Alexander M. Hainen
Purdue University, ahainen@eng.ua.edu

Stephen M. Remias
Purdue University, sremias@wayne.edu

Hiromal Premachandra
Purdue University

See next page for additional authors

Reliability, Flexibility, and Environmental Impact of Alternative Arterial Offset Optimization Objective Functions

by

Christopher M. Day
Purdue University

Thomas M. Brennan, Jr.
Purdue University

Alexander M. Hainen
Purdue University

Stephen M. Remias
Purdue University

Hiromal Premachandra
Purdue University

James R. Sturdevant
Indiana Department of Transportation

Greg Richards
Indiana Department of Transportation

Jason S. Wasson
Indiana Department of Transportation

Corresponding author:
Darcy M. Bullock
Purdue University
550 Stadium Mall Dr
West Lafayette, IN 47906
Phone (765) 496-2226
Fax (765) 496-7996
darcy@purdue.edu

March 15, 2011

TRB Paper No. 11-0036

Word Count: 4935 words + 10 x 250 words/Figure-Table = 4935 + 2500 = **7435**

ABSTRACT

A wide variety of alternative optimization objective functions have been reported in the literature such as minimizing stops, minimizing delay, and maximizing arrivals on green. There is extensive literature evaluating these alternative objective functions using models. This paper reports on the field deployment of these alternative optimization functions, developed using high resolution controller data, to adjust offsets on an arterial system of eight coordinated signals. The deployment consisted of a one-week base data collection, and four one-week deployments of offset plans developed using four alternative optimization objective functions. Anonymous probe vehicle travel times were measured during the study period to evaluate the impact of these alternative optimization functions on corridor travel time. All of the objective functions were successful in significantly reducing median corridor travel time. Median travel time decreased by more than one minute in both directions on the 5-mile corridor. Travel time reliability, as quantified by the difference between 75^{th} and 25^{th} percentile travel times, was improved for the busiest portion of the day. A lower bound on the estimated annual user cost savings was estimated at $472,817 with an associated reduction in CO_2 emissions of 197 tons per year.

INTRODUCTION

With over 350,000 traffic signals in operation in the US, signal timing has a considerable impact on the performance of the roads and streets that they control, directly influencing their ability to provide mobility to users, and their environmental impact (*1*). It is important for agencies to assess and improve signal timing plans, but often difficult to allocate necessary resources. It is therefore highly desirable to measure the effects of signal timing to communicate the necessity of the activity and to support and promote investment in signal operations.

Signal offsets are typically designed by software packages that optimize offsets according to one of several mathematical objectives. One strategy is to *maximize bandwidth* (*2,3,4,5,6,7,8*). Another major strategy is *minimize disutility,* such as delay (*9,10,11*). TRANSYT is a well known disutility-minimizing optimization procedure based on a macroscopic traffic model (*11,12*). Similar concepts have also been used in adaptive systems such as SCOOT (*13, 14*) and OPAC (*15,16,17,18*). A related objective that has been used in adaptive systems is to *maximize arrivals on green* (*19,20,21*). This is a simple calculation requiring fewer assumptions than delay models, making it ideal for real-time calculation. Although proposed for adaptive systems, green arrival maximization could also be used in offline offset optimization. This paper investigates whether green arrival maximization and disutility minimization yield comparable results in the field.

In a previous study, Jovanis and May (*22*) compared alternative objectives within TRANSYT-6C that effectively considered optimizing for vehicles against optimizing for the number of passengers. They concluded that minimizing passenger delay and minimizing fuel consumption were the most effective objective functions. The alternative objectives were evaluated within the macroscopic TRANSYT-6C model. A subsequent study by Leonard and Rodegerdts (23) tested 10 alternative objectives obtained from TRANSYT-7F and PASSER II-90 by modeling in TRANSYT-7F. Among other findings, it was observed that the system-wide average speeds did not vary by objective. Explicitly optimizing for minimum delay yielded the lowest delay, but

there was relatively little variation in delay among the 10 objectives, for most of the different scenarios tested in the study.

Recently, it was demonstrated that green arrival maximization could be used to improve offsets in an off-line procedure (*24*), and that the optimization procedure results can be similar to delay minimization (*25*,*26*). This paper follows up to those studies, expanding the comparison to four objectives, including two that minimize disutility, and two that maximize green arrivals. The post-implementation outcomes are presented in terms of arterial travel times measured on an eight-intersection arterial.

METHODOLOGY

Objective Functions

The chief tool used to optimize offsets in this study is the *cyclic flow profile*. A profile is designated for each coordinated signal approach for a given analysis period, and represents arrival conditions for an "average cycle" over an analysis period. Figure 1(a) shows an example flow profile, with a superimposed probability of green under actuated-coordinated operations. In this example, each bin represents two seconds. This profile view is equivalent to those provided by TRANSYT (with the exception of the probabilistic green) and ACS-Lite. In this study, both the probability of green and the arrival profile were determined from observed signal event data. For example, the probability of green for any bin is equal to the percentage of observed cycles for which an effective green state was active at that time in the cycle. Similarly, the number of vehicles arriving for any bin is simply the sum over all observed cycles of the number of vehicles detected at that time in the cycle.

Figure 1(b) shows the estimated number of queued vehicles based on the observed arrivals and the departures implied by the probability of green. Starting from the end of the green band, vehicles that arrive during red are assumed to join the queue, which grows until the beginning of green. After the beginning of green (and accounting for start-up lost time), vehicle departures reduce the queue size until it disperses. The number of queued vehicles for a given bin is equal to

$$q_i = \max\left(0, \quad q_{i-1} + N_i - c_i\right), \qquad \text{Equation 1}$$

where q_i is the queue length of the i^{th} bin, N_i is the number of vehicle arrivals associated with the bin, and c_i is the capacity or maximum number of departures in the bin, obtained from the probability of green G_i, number of cycles Q, and saturation flow rate s from

$$c_i = sQG_i . \qquad \text{Equation 2}$$

The total delay incurred by the vehicles is equal to the summation of the queue size, which gives the area between the arrival and departure profiles:

$$d = w\sum_i q_i . \qquad \text{Equation 3}$$

Here, w is the bin width in seconds. The number of stops can be found by making a few additional assumptions based on the queue profile and probability of green. We assume that vehicles that arrive during a particular time in cycle will stop if a queue exists, or if the signal is red. Specifically, the number of stops per bin is calculated by:

$$S_i = \begin{cases} N_i, & \text{if } q_i > 0 \\ N_i\left(1 - G_i\right) & \text{if } q_i = 0 \end{cases} \qquad \text{Equation 4}$$

Here, $(1 - G_i)$ represents the probability of the signal being red. A composite performance index combining both delay and stops can be specified as follows.

$$PI = d + k\sum_i S_i \,, \qquad \text{Equation 5}$$

Here, k is a weighting factor that converts stops into an equivalent number of seconds of delay. This is similar to the PI used by early versions of TRANSYT (*11*). For this study, a value of k = 20 was used, which put the value of the total stops on the same order of magnitude as the total delay.

The flow profile in Figure 1(a) can also be used to calculate the number of arrivals on green (N_g):

$$N_g = \sum_i G_i N_i \,. \qquad \text{Equation 6}$$

This is the portion of the vehicle profile captured by the green band. The calculation is equivalent to taking the vector dot product of G_i and N_i.

The number of arrivals on green is a simple calculation, but it does not intrinsically consider vehicle queuing. It seems likely that offsets designed to maximize N_g may give insufficient time to clear standing queues before coordinated platoons arrive. To mitigate this limitation, we propose an alternative objective, in which a portion of time at the beginning of the green band is considered to be part of "red" during optimization. Ideally, this would ensure that a certain portion of green is provided to clear queues before the heaviest portion of the platoon arrives. The objective is illustrated by Figure 1(c). Here, the first ten seconds (five bins) of the green band are considered to be "red" by the optimization process (i.e., they are excluded from Equation 6). The 10-second value was selected because it is not excessive compared to a typical arterial split (approximately 40-50 seconds), yet provides enough time to clear about 5 vehicles per lane after the start of effective green. It is proposed in this paper as a proof of concept because it was appropriate for the traffic scenario on the test arterial.

To summarize, this paper examines the outcomes of the four objectives defined above:

- Objective I. Minimize delay (Equation 3).
- Objective II. Minimize delay and stops (Equation 5).
- Objective III. Maximize arrivals on green. (Equation 6)
- Objective IV. Maximize arrivals on green with queue clearance time (Figure 1(c)).

Example for One Coordinated Approach

To optimize offsets, we must identify a model for predicting performance under different offsets. In this study, we use observed data to establish a baseline, and model performance under various offset adjustments by appropriately shifting the arrival profiles. For example, to model a 10 second adjustment of the offset of an *upstream* intersection, we would move the arrival distribution forward by 10 seconds. A *local* offset adjustment of 10 seconds is modeled by moving the green distribution forward by 10 seconds, or equivalently by moving the arrival data in the opposite direction. It is assumed that the vehicle arrival distributions are not changed by the offset adjustment. This model is equivalent to that used by Abbas *et al*. (*19*), ACS-Lite (*20*), and in a prior study with similar field data (*21*, *24*). The idea descends from the technique used by Hillier and Rothery (*9*) to populate delay-offset curves by superimposing an expected green profile over a measured arrival profile at all possible offset values.

Figure 2 shows an example of a sweep through a 104-second cycle length for possible values of local offset for a coordinated approach. Seven views of the sweep at 15-second spacing are displayed. In this example, the arrival distribution is moved relative to the probability of green; the results remain the same regardless of how the adjustment is implemented. The movement of arrivals and the change in the resulting estimated queues are shown by the second and third columns in the figure, with the superimposed green line showing the probability of green.

The probability of green distribution takes on a distinctive shape related to early return to the coordinated phase resulting from side street phase omits and early termination (Figure 2, Callout "A"), and the occasional extension of the coordinated green ("B") associated with the use of a controller feature allowing the coordinated phase to be extended by up to 10% of the cycle (*27*), or to terminate and yield the time to other phases during low utilization. The shape of the vehicle arrival distribution related to upstream signal operations. A large platoon due to the coordinated phase is the prominent feature ("C"), while the presence of a secondary platoon ("D") resulting from upstream left and right turns can also be observed. Queue sizes are shown in the third column. As expected, we see queues accumulating with vehicle arrivals in red, and they disperse after the beginning of green ("E").

The optimum offset value varies according to the objective function selected. Figure 3 shows graphs of the four objective functions under evaluation through the range of possible adjustments to the offset, with Objectives I, II, III, and IV shown respectively by Figure 3(a), Figure 3(b), Figure 3(c), and Figure 3(d). The curves were obtained from the data shown in Figure 2. The value of the objective functions for a given offset corresponds to a superposition of the vehicle arrival and probability of green profiles. All four optimal offsets fell within a 14 second range. The optimal region is largely coincident between the four objectives; the remainder of this paper investigates whether the cumulative effects of optimizing several intersections together leads to any substantial difference in arterial performance for different objectives.

To understand the reason for differences between the outcomes in the example case, the optimal flow profiles are displayed in Figure 4.

- In Figure 3(a), a region from approximately +40 to +60 is clearly the optimal offset region, but the minimum delay occurs at +56. The flow profile in Figure 4(a) shows that this has placed the platoon slightly before the start of green. Vehicles that arrive shortly after the end of green accumulate much more delay than those arriving a few seconds prior to the start of green, because they have to wait through the entire red interval. Consequently, minimizing for delay alone tends to schedule platoons to arrive early rather than be cut off.
- Minimizing delay and stops and maximizing N_g both resulted in the same optimal offset adjustment of +44. In Figure 4(b), it is clear that this is the region where the largest portion of the vehicle arrivals are coincident with the green indication. It would seem that adding stops to delay counters the tendency of delay minimization to make vehicles arrive slightly prior to the start of green.
- In Objective IV, the alternative max N_g, the first ten seconds of green are excluded from the optimization process. This results in a more narrow optimal region, as shown in Figure 3(c). The actual and optimal green bands are shown in Figure 4(c) respectively by the green line and the shaded region. This objective is intended to create a period of green time with few arrivals prior to the primary platoon, in order to clear standing queues.

Optimizing network offsets is a complex task because of interactions between offsets on a system. A variant of the Combination Method algorithm (*10*) was used to search for optimal offsets. This algorithm was selected because it systematically provided consistent, optimal offsets in less time than other algorithms. The procedure is summarized as follows. Starting from one end of the arterial, the offset at each successive intersection is adjusted until the optimal value of the performance measure is obtained for the two links controlled by the offset. When moving to the next intersection, the previously optimized link flows are held constant by adjusting all preceding offsets by the same value as the current offset adjustment. The procedure

continues until the entire arterial has been optimized. For further detail, we refer the reader to more extensive documentation available elsewhere (*25, 26, 28*).

STUDY CORRIDOR

The test arterial used in this study is SR 37 in Noblesville, Indiana (*25*,*26*,*27*). A map of the system is provided in Figure 5. This 5.2-mi (8.3 km) corridor consists of eight coordinated intersections that operate a common cycle length. Vehicle detectors are located on all arterial through lanes at a distance of 405 ft back from the stop bar. Vehicle detection times were adjusted by 5 seconds to account for travel time from the advance detector to the stop bar. At each intersection, a log-capable signal controller was deployed to collect signal event data at a resolution of 0.1 seconds (*29*). Additionally, anonymous probe vehicle travel time measurements were obtained from Bluetooth (BT) device MAC address matching (*24*,*30*,*31*,*32*) using cases deployed at the entry points and at one midpoint location in the system. From this arrangement, it was possible to obtain travel time measurements for the entire arterial (Case A to Case C), and for two smaller systems, System 1 (Case A to Case B) and System 2 (Case B to Case C).

For this paper, we focus on outcomes for the Saturday time-of-day (TOD) plan, which runs from 0600-2200. The Saturday timing plan was selected because it was the focus of prior offset study in 2009 (*24*) for System 1, and because the offsets in System 2 were known to be suboptimal. On Saturdays, SR 37 carries approximately 30,000 vehicles per day in both directions. Demand is moderate and roughly steady between 9:00 and 18:00. For this reason, one timing plan is used for the entire day.

To optimize this 16-hour TOD plan, sixteen one-hour flow profiles per approach were constructed. The objective functions calculated independently for the sixteen one-hour flow profiles were then summed to obtain the value for the approach for the entire time of day. In a previous study, optimization outcomes from a smaller sub-portion of the day were found to be very similar to those for the entire sixteen-hour period (*26*). Baseline data from Saturday, May 29, 2010 was used for optimization. The resulting offsets for the four alternative optimization objectives were subsequently deployed in the field throughout June and July 2010.

RESULTS

Arterial Signal Progression

Flow profiles for the baseline offsets and optimal offsets from Objective III (maximize arrivals on green) are shown in Figure 6 to illustrate signal operations before and after implementation of optimal offsets procedure. There is not enough space to show the observed post-implementation flow profiles for the other three objectives, but they were similar to the outcomes of Objective III, with differences along the same lines as those presented for one approach in Figure 4.

Most of the improvement in the system was achieved in System 2 (Ints. 5,6,7,8). This is not unexpected, because the offsets in System 1 (Ints. 1,2,3,4) had been optimized about one year prior to this study (*24*). The baseline observed flow profiles confirmed our anecdotal knowledge of sub-optimal offsets in System 2. Specifically, the northbound movement at Int. 5 and the southbound movement at Int. 6 both have platoons arriving almost completely outside of the green bands. This was corrected by the optimization procedure. More modest changes were suggested for other intersections, leading to smaller shifts in platoon arrivals. The effects of these adjustments on arterial performance are described in the next section.

Changes in Arterial Travel Time and Travel Time Reliability

To analyze the travel time results, three-hour intervals beginning at 0600, 0900, 1200, 1500, and 1800 were used to group samples. Three hours was a long enough time period to obtain a large number of samples, but short enough to observe any potential differences in travel time characteristics between different times of day.

Figure 7 shows cumulative frequency diagrams (CFDs) of the 1500-1800 interval for Saturdays during the baseline and while operating under four offset optimization objectives. The four lines in each plot are listed by objective number. The CFDs illustrate the movement of the central tendency of the travel time as the change in the median. If reliability is characterized as consistency in travel times, then greater consistency is associated with less variation in the

measured travel times. In the CFD, this appears as a steeper line with a smaller interquartile range (IQR), the distance between the 25th percentile and the 75th percentile. Detailed numbers are shown in Table 1 for several time periods, including 1500-1800.

- CFDs of travel times along the entire arterial are shown for Southbound vehicles in Figure 7(a) and Northbound vehicles in Figure 7(b). For this path, all four objectives clearly improved travel times compared to the baseline, with median travel times decreasing by approximately a minute. Obj. II did not perform as well as the others (there was a slight increase in southbound travel time in System 1, as discussed below), but still yielded a net improvement for the arterial, while the traces for the other three objectives are almost identical. For southbound traffic, the reliability seems to have improved (i.e., the slope of the optimized traces are steeper than the baseline).
- CFDs for travel times through System 1 are shown in Figure 7(c) Figure 7(d) respectively for southbound and northbound vehicles. There is not much improvement in travel times compared to the baseline (in fact, Obj. II saw an increase in travel time for southbound vehicles). As mentioned before, offsets in this part of the arterial were already near optimal. However, the reliability for northbound vehicles has improved somewhat; the shape of the baseline curve in Figure 7(d) shows a plateau in the curve, a greater IQR. The other traces still exhibit a plateau, but it contains a much smaller portion of the observed vehicles.
- CFDs for travel times through System 2 are shown in Figure 7(e) Figure 7(f) respectively for southbound and northbound vehicles. This portion of the system had not been retimed in several years, and was known to have suboptimal offsets at two intersections. Consequently, a substantial improvement in travel times was achieved by all four objectives.

It is clear that optimizing offsets reduces overall arterial travel time. We hypothesize that optimizing offsets should have a beneficial impact on the *reliability* of travel time. In Table 1, for the 1500-1800 time period we see that IQR decreased (comparing the baseline to optimized offsets under four objectives), for most of the objectives in both directions. Similar improvements are not observed in other time periods, especially the 0600-0900 and 1800-2100

shoulder periods when traffic volumes are decreased. With a few exceptions, IQR decreased for the 0900-1200 and 1200-1500 time periods, where traffic volumes are relatively higher. The results suggest that offset optimization can positively impact travel time reliability, but the results do not show that any particular optimization objective has a better outcome than the others.

Note that the CFDs for System 2 [Figure 7(e), Figure 7(f)] exhibit more consistent travel times than System 1 [Figure 7(c), Figure 7(d)]. That is, the slope of the CFDs are steeper for System 2 and the IQR is smaller than that of System 1. This is attributable to differences in the characteristics of the two systems. Both systems have similar access control and traffic mix; one potential reason for the difference could be the road geometry. System 2 is a straight road and the distances between intersections are either 2650 or 5320 ft (nearly perfect regular spacing). System 1, on the other hand, has some curvature and less regular spacing.

Flexibility: Sensitivity to Time of Day

Comparing the performance across time periods characterizes the flexibility of the plan, or its ability to tolerate variations in traffic patterns throughout the day and provide similar performance for both northbound and southbound vehicles. The Saturday signal timing plan covers a 16-hour TOD interval. Often, offsets are designed to treat a certain direction preferentially by time of day. In this study, no weighting was given to any particular movement. It is desirable to determine whether this scheme caused either movement to suffer during particular times of day.

Figure 8 illustrates these fluctuations in box-whisker plots of travel times for the baseline offsets and the four optimized offsets. These are shown in five graphs representing five three-hour analysis subperiods. In each column, the line represents the range between the minimum and maximum values, with a marker showing the median value, while the box displays the 25^{th} and 75^{th} percentiles (and hence the IQR). Figure 8(a) shows travel times for northbound vehicles while Figure 8(b) shows travel times for southbound vehicles. Detailed information corresponding to these graphs are also presented in Table 1.

During most times of day, the median travel times were reduced by the optimized offsets, representing a net improvement in arterial ravel time. For example, from 1500-1800, northbound travel times improved from 1.2–1.6 minutes and southbound travel times improved by 0.6–1.1 minutes, varying by objective. During several time periods, the IQR also decreased, indicating that the reliability of travel time improved. This is true of northbound vehicles during most time periods for nearly all objectives [Figure 8(a)], agreeing with earlier observations from the CFDs. These trends are observed in both northbound and southbound direction for all time periods with the exception of 0600-0900. The reason for lack of improvement in the early morning is that side street volumes are sufficiently that the arterial movements enjoy extended green times (because of fewer minor phase actuations) during *both* the baseline and all four optimized scenarios.

Both Figure 8(a) and Figure 8(b) illustrate increasing an increase in median travel times around 1200-1500 compared to the other time periods. Northbound and southbound travel times are more similar after optimization than the baseline case. For example, from Table 1, during the 1200-1500 time period, under the baseline offsets the median northbound travel time was 1.4 min greater than the southbound travel time (11.2 versus 9.8 min). With optimal offsets, the difference between median northbound and southbound travel times decreased, with the magnitude of the decrease varying by objective. For example, under Obj. II, northbound travel times were only 0.1 min longer than southbound travel times, while Obj. III was less flexible, with a 1.0-min difference between the two. Similar changes can be observed in the other time periods.

Table 1 provides several statistical measures in addition to the median travel time and the IQR. An alternative measure of central tendency are the mean and standard deviations. We have highlighted the median and IQR because they are directly related to the CFDs and box-whisker plots and are less sensitive to outliers. However, similar trends are observable in the mean and standard deviation. Table 1 also displays the results of a t-test between the baseline offsets and the four optimized offsets. With the exceptions of the 0600-0900 time period, and for Objective II during 1500-1800, the *t*-test revealed statistically significant changes in travel time, with P-values showing confidence above the 95% level in all cases, and above 99% for most.

User Benefit Estimation

The following equations were applied to establish a method for comparing the optimized arterial travel time (TT) to a base travel time:

$$\Delta TT = TT_{Base(\text{section})} - TT_{Objective(\text{section})}, \qquad \text{Equation 7}$$

where $TT_{Base(section)}$ was the arterial travel time measured in minutes for a specified section (Figure 5, System 1 or System 2) and direction (northbound, southbound) running baseline offsets and $TT_{Objective(section)}$ was is the travel time for each section, after optimal offsets were implemented. The cost estimation methodology presented here is based on the 2009 Transportation Urban Mobility Report (*33*). Costs for *trucks* are given by

$$USER_t = \Delta TT * Vol * \%T * PPV_t * \frac{\$102.12}{\text{hr}} * \frac{1\,\text{hr}}{60\,\text{min}}, \qquad \text{Equation 8}$$

where $USER_t$ is the user cost for a commercial vehicle, *Vol* is the volume (number of vehicles) measured for the study period, %*T* is the percentage of commercial trucks (2% for Saturday), and PPV_t is the number of passengers per vehicle (1 for commercial trucks). The $102.12 amount represents the time value of money for commercial vehicles and is taken from the 2009 Transportation Urban Mobility Report (*33*). This value does not reflect excess fuel consumption. When ΔTT is positive, the outcomes of the equation reflect a user savings. Costs for passenger cars are given by

$$USER_c = \Delta TT * Vol * \%C * PPV_c * \frac{\$15.47}{\text{hr}} * \frac{1\,\text{hr}}{60\,\text{min}}, \qquad \text{Equation 9}$$

where $USER_c$ is the user cost for a passenger vehicle, %*C* is the assumed percentage of passenger vehicles (98% for Saturday), PPV_c is assumed to be 1.2, and a lower time value of money at $15.47 per hour (*33*) is applied.

In addition to user costs, potential savings in fuel consumption and associated changes in CO_2 emissions can be derived from the following equations.

$$FUEL = \Delta TT * Vol * \frac{0.87\,\text{gal}}{\text{hr}} * \frac{1\,\text{hr}}{60\,\text{min}}, \qquad \text{Equation 10}$$

In Equation 10, *FUEL* is the change in the amount of fuel consumed (gallons), which is a savings when ΔTT is positive. Using conversion factors from Argonne National Laboratory, a passenger car that idles at 1,000 rpm with air conditioning on 50% of the time can be expected to consume 0.87 gallons of gasoline per hour, or 0.0145 gallons per minute (*34*, *35*). This number was used to conservatively estimate the change in fuel consumption for all vehicle types associated with changes in travel time. For decreases in travel time (positive ΔTT), the amount of CO_2 emissions that are prevented are calculated from the following two equations:

$$CO_2 = FUEL * \frac{19.4\,\text{lbs}}{\text{gal}} * \frac{1\,\text{ton}}{2000\,\text{lbs}}, \qquad \text{Equation 11}$$

$$CC = CO_2 * \frac{\$22}{\text{ton}}, \qquad \text{Equation 12}$$

Here, *CC* represents the "CO_2 cost." According to the EPA, the amount of CO_2 emitted when a gallon of gasoline burns is approximately 19.4 lbs/gallon (*36*). The monetary equivalent of the CO_2 is assumed to be approximately \$22/ton of CO_2 produced (*37*).

The results shown in Table 2 illustrate the benefit for system users based on above analysis. The savings is calculated from changes in arterial travel time measured with anonymous probe vehicles, and volumes measured using vehicle counts logged in the signal event data. By optimizing Saturday offsets, user cost reductions ranging from \$471,817 (Objective III) to \$600,073 (Objective IV) could be realized, depending on which offsets are permanently implemented. The associated reduction in CO_2 emissions was found to range from 197 to 250 tons of CO_2 per year.

CONCLUSIONS

This paper developed and independently validated the benefits of offset optimization for several objectives using directly measured vehicle travel times to quantify delay, user cost savings, and environmental impact. Four optimization objectives were identified: minimize delay; minimize a performance index based on delay and stops; maximize arrivals on green; and maximize arrivals on green, with 10 seconds of queue clearance time at the beginning of green. The results for all four objectives were quite similar. For an individual coordinated approach, the optimal offsets were found to coincide within a 14 second range inside of a 114 second cycle length (Figure 3). When scaled to an eight-intersection corridor, the overall outcomes in terms of the travel time and travel time reliability were also rather similar (Table 1). The outcomes of the delay-based optimization objectives were generally close to the outcomes of green arrival maximization, as shown in Table 2 and in several performance measure graphics (Figure 7, Figure 8). These results demonstrate that green arrival maximization can be used to effectively optimize offsets with a similar level of benefit as derived from delay minimization.

This paper demonstrated the use of anonymous probe vehicle travel time data in describing changes in travel time as well as the reliability of travel time, and additionally showed how that data can be translated into user cost savings and environmental benefits. In this case study, a lower bound on the estimated benefits was calculated at approximately $470,000. Measured travel time results are a compelling tool to communicate the value of investments in traffic signal systems to the public and to elected decision makers. This information is essential to obtain and communicate, particularly for improvements in operations such as signal retiming that have relatively low visibility compared to construction, but can nevertheless have substantial environmental and economic impacts.

ACKNOWLEDGMENTS

This work was supported by the National Cooperative Highway Research Program under project NCHRP 3-79A, and by the Joint Transportation Research Program administered by Purdue University and the Indiana Department of Transportation. The contents of this paper reflect the views of the authors, who are responsible for the facts and the accuracy of the data presented herein, and do not necessarily reflect the official views or policies of the sponsoring organizations. These contents do not constitute a standard, specification, or regulation.

REFERENCES

1. Peters, J., R. McCourt, and R. Hurtado. "Reducing Carbon Emissions and Congestion by Coordinating Traffic Signals." *ITE Journal*, Vol. 79, No. 4, pp. 25-29, April 2009.

2. Morgan, J.T. and J.D.C. Little. "Synchronizing Traffic Signals for Maximal Bandwidth." Operations Research, Vol. 12, pp. 896-912, 1964.

3. Little, J.D.C., M.D. Kelson, and N.H. Gartner. "MAXBAND: A Program for Setting Signals on Arteries and Triangular Networks." *Transportation Research Record No. 795*, TRB, National Research Council, Washington, DC, pp. 40-46, 1981.

4. Messer, C.J., R.H. Whitson, C.L. Dudek, and E.J. Romano. "A Variable Sequence Multiphase Progression Optimization Program." *Highway Research Record No. 445*, pp. 24-33, 1973.

5. Messer, C.J., H.E. Haenel, and E.A. Koeppe. "A Report on the User's Manual for Progression Analysis and Signal System Evaluation Routine—Passer II." Texas Transportation Institute Report No. TTI-218-72-165-14, Texas Transportation Institute, Texas A&M University, College Station, TX, 1974.

6. Gartner, N.H., S.F. Assmann, F. Lasaga, and D.L. Hou. "MULTIBAND – A Variable-Bandwidth Arterial Progression Scheme." *Transportation Research Record No. 1287*, pp. 212-222, 1990.

7. Tsay, H.-S. and L.-T. Lin. "A New Algorithm for Solving the Maximum Progression Bandwidth." In *Transportation Research Record No. 1194*, pp. 15-30, 1988.

8. Yin, Y., M. Li, and A. Skabardonis. "Offline Offset Refiner for Coordinated Actuated Signal Control Systems." ASCE Journal of Transportation Engineering, Vol. 133, No. 7, pp. 423-432, 2007.

9. Hillier, J.A. and R. Rothery. "The Synchronization of Traffic Signals for Minimum Delay." Transportation Science, Vol. 1, pp. 81-94, 1967.

10. Hillier, J.A. "Appendix to Glasgow's Experiment in Area Traffic Control." Traffic Engineering and Control, Vol. 7, No. 9, 1966.

11. Robertson, D.I. " 'TRANSYT' Method for Area Traffic Control." Traffic Engineering and Control, Vol. 11, pp. 276-281, 1969.

12. Robertson, D.I. *Transyt: a Traffic Network Study Tool.* Report No. LR 253, Road Research Laboratory, Crowthorne, Berkshire, England, 1969.

13. Hunt, P.B., D.I. Robertson, R.D. Bretherton, and R.I. Winton. SCOOT- A Traffic Responsive Method of Coordinating Signals. Report No. LR 1014, Transport and Road Research Laboratory, Crowthorne, Berkshire, England, 1981.

14. Robertson, D.I. and R.D. Bretherton. "Optimizing Networks of Traffic Signals in Real Time—The SCOOT Method." IEEE Transactions on Vehicular Technology, Vol. 40, No. 1, pp. 11-15, 1991.

15. Gartner, N.H. "OPAC: A Demand-Responsive Strategy for Traffic Signal Control." In *Transportation Research Record No. 906*, Transportation Research Board of the National Academies, Washington, DC, pp. 75-81, 1983.

16. Gartner, N.H., P.J. Tarnoff, and C.M. Andrews. "Evaluation of Optimized Policies for Adaptive Control Strategy." In *Transportation Research Record No. 1344*, Transportation Research Board of the National Academies, Washington, DC, pp. 105-114, 1991.

17. Gartner, N.H. *Demand-Responsive Decentralized Urban Traffic Control. Part I: Single-Intersection Policies*. Report No. ULRF-05-2998-1, University of Lowell Research Foundation, Lowell, Massachusetts, February 1982.

18. Gartner, N.H., M.H. Kaltenbach, and M.M. Miyamoto. *Demand-Responsive Decentralized Urban Traffic Control. Part II: Network Extensions*. Report No. ULRF-05-2998-2, University of Lowell Research Foundation, Lowell, Massachusetts, July 1983.

19. Abbas, M., D. Bullock, and L. Head. "Real-Time Offset Transitioning Algorithm for Coordinating Traffic Signals." In *Transportation Research Record No. 1748*, Transportation Research Board of the National Academies, Washington, DC, pp. 26-39, 2002.

20. Luyanda, F., D. Gettman, L. Head, S. Shelby, D. Bullock, and P. Mirchandani. "ACS-Lite Algorithmic Architecture: Applying Adaptive Control System Technology to Closed-Loop Systems." In *Transportation Research Record No. 1856*, Transportation Research Board of the National Academies, Washington, DC, pp. 175-184, 2003.

21. Gettman, D., S.G. Shelby, L. Head, D. Bullock, and N. Soyke. "Data-Driven Algorithms for Real-Time Adaptive Tuning of Offsets in Coordinated Traffic Signal Systems." In *Transportation Research Record No. 2035*, Transportation Research Board of the National Academies, Washington, DC, pp. 1-9, 2007.

22. Jovanis, P.P. and A.D. May. "Alternative Objectives in Arterial-Traffic Management." *Transportation Research Record No. 682*, Transportation Research Board of the National Academies, Washington, DC, pp. 1-8, 1978.

23. Leonard, J.D. and L.A. Rodegerdts. "Comparison of Alternative Signal Timing Policies." *Journal of Transportation Engineering*, Vol. 124, pp. 510-520, 1998.

24. Day, C.M., R. Haseman, H. Premachandra, T.M. Brennan, J.S. Wasson, J.R. Sturdevant, and D.M. Bullock. "Visualization and Assessment of Arterial Progression Quality Using High Resolution Signal Event Data and Measured Travel Time." Transportation Research Board Annual Meeting, Paper No. 10-0039, Transportation Research Board of the National Academies, Washington, DC, 2010.

25. Day, C.M. *Performance-Based Management of Arterial Traffic Signal Systems.* PhD Thesis, Purdue University, May 2010.

26. Day, C.M., and Bullock, D.M. *Arterial Performance Measures, Volume 1: Performance-Based Management of Arterial Traffic Signal Systems*. NCHRP 3-79A Report, National Cooperative Highway Research Program, Transportation Research Board, Washington, DC, under review, to appear 2010.

27. Day, C.M., E.J. Smaglik, D.M. Bullock, and J.R. Sturdevant, (2008). "Quantitative Evaluation of Actuated Coordinated Versus Nonactuated Coordinated Phases," *Transportation Research Record No. 2080*, TRB, National Research Council, Washington, D.C., pp. 8-21.

28. Day, C.M. and D.M. Bullock. "Evaluation of Alternative Algorithms for Traffic Signal Offset Optimization Using High Resolution Event Data." Submitted to Transportation Research Record, July 31, 2010.

29. Smaglik, E.J., Sharma, A., Bullock, D.M., Sturdevant, J.R., and Duncan, G. "Event-Based Data Collection for Generating Actuated Controller Performance Measures." *Transportation Research Record No. 2035*, Transportation Research Board of the National Academies, Washington, DC, pp. 97–106, 2007.

30. Wasson, J.S., J.R. Sturdevant, D.M. Bullock, "Real-Time Travel Time Estimates Using MAC Address Matching," *Institute of Transportation Engineers Journal*, ITE, Vol. 78, No. 6, pp. 20-23, June 2008.

31. Tarnoff, P.J., J.S. Wasson, S.E. Young, N. Ganig, D.M. Bullock, and J.R. Sturdevant. "The Continuing Evolution of Travel Time Data Information Collection and Processing," Transportation Research Board Annual Meeting, Paper No. 09-2030, Transportation Research Board of the National Academies, Washington, DC, 2009.

32. Brennan, T.M., J.M. Ernst, C.M. Day, D.M Bullock, J.V. Krogmeier, and M. Martchouk. "Influence Of Vertical Sensor Placement On Data Collection Efficiency From Bluetooth MAC Address Collection Devices," Paper No. TEENG-418, submitted to Journal of Transportation Engineering, ASCE, May 2009.

33. Schrank, D., and T. Lomax, The 2009 Urban Mobility Report. Texas Transportation Institute, July, 2009.

34. "Analysis of Costs from Idling and Parasitic Devices for Heavy Duty Trucks," Technology and Maintenance Council Recommended Practice Bulletin 1108. Issued March 1995, reprinted 2003 by TMC/ATA.

35. Lutsey, N.P., J.P. Wallace, C.J. Brodrick, H.A. Dwyer, and D. Sperling, "Modeling Auxiliary Power Options for Heavy-Duty Trucks: Engine Idling vs. Fuel Cells." Society of Automotive Engineers Report No. 2004-01-1479, October 2004.

36. Emission Facts: Greenhouse Gas Emissions from a Typical Passenger Vehicle EPA420-F-05-004 February 2005, http://www.epa.gov/OMS/climate/420f05004.htm, Accessed July 27, 2010.

37. EPA Analysis of the American Clean Energy and Security Act of 2009 , H.R. 2454 in the 111th Congress, http://www.epa.gov/climatechange/economics/pdfs/HR2454_ Analysis.pdf Accessed July 27, 2010.

List of Tables

List of Figures

Table 1. Arterial travel time (Case A to Case C) Statistics,
Saturdays, 3-hour analysis periods, with alternative offsets in use.

		Southbound					Northbound				
Time	MOE	Baseline	Obj. I	Obj. II	Obj. III	Obj. IV	Baseline	Obj. I	Obj. II	Obj. III	Obj. IV
Saturday 0600-0900	25 %	7.5	7.0	6.9	7.4	7.2	6.5	7.2	6.9	6.9	7.0
	Median	**8.4**	**7.4**	**7.6**	**8.1**	**8.4**	**6.8**	**7.7**	**7.4**	**7.5**	**7.1**
	75 %	9.1	8.0	8.2	8.5	11.2	7.7	8.1	8.1	8.3	8.0
	IQR	**1.6**	**1.0**	**1.3**	**1.1**	**4.0**	**1.2**	**0.9**	**1.3**	**1.5**	**1.0**
	Mean	8.2	7.8	7.9	8.2	9.1	7.3	7.7	7.4	8.1	7.4
	St. Dev.	1.3	1.6	1.7	1.4	2.1	1.6	1.0	0.9	2.0	1.0
	N	10	22	22	19	9	19	26	11	16	10
	t-value		-0.64	-0.51	0.05	1.24		1.01	0.20	1.29	0.05
	P-value		0.527	0.614	0.957	0.232		0.318	0.842	0.208	0.960
Saturday 0900-1200	25 %	9.2	8.1	7.6	8.0	7.4	8.5	7.6	7.5	7.0	7.2
	Median	**9.9**	**8.7**	**8.3**	**8.4**	**7.7**	**9.1**	**8.4**	**8.1**	**7.5**	**7.5**
	75 %	10.8	9.6	9.1	9.2	9.7	10.1	8.9	8.8	8.0	8.2
	IQR	**1.6**	**1.6**	**1.5**	**1.2**	**2.3**	**1.6**	**1.3**	**1.3**	**0.9**	**1.0**
	Mean	10.2	8.9	8.6	8.6	8.6	9.5	8.4	8.3	7.5	7.8
	St. Dev.	1.2	1.2	1.5	1.1	1.9	1.7	1.3	1.1	0.5	1.1
	N	29	40	39	32	33	25	36	39	22	30
	t-value		-4.67	-4.77	-5.42	-3.87		-2.93	-3.67	-5.56	-4.65
	P-value		<0.001	<0.001	<0.001	<0.001		0.005	0.001	<0.001	<0.001
Saturday 1200-1500	25 %	9.9	8.3	8.5	9.1	8.1	9.1	8.0	8.1	8.1	8.0
	Median	**11.2**	**9.4**	**8.9**	**9.8**	**9.1**	**9.8**	**8.7**	**8.8**	**8.8**	**8.7**
	75 %	12.3	10.2	9.8	10.6	10.0	10.5	9.9	10.0	9.4	9.0
	IQR	**2.4**	**1.9**	**1.2**	**1.5**	**1.9**	**1.4**	**1.9**	**2.0**	**1.3**	**1.0**
	Mean	11.2	9.4	9.0	9.9	9.3	9.8	9.0	9.0	8.9	8.5
	St. Dev.	1.6	1.3	1.0	1.5	1.7	0.8	1.4	1.2	1.2	1.0
	N	25	34	34	31	44	30	34	28	42	25
	t-value		-4.86	-6.62	-3.25	-4.47		-2.54	-2.94	-3.41	-5.19
	P-value		<0.001	<0.001	0.002	<0.001		0.014	0.005	0.001	<0.001
Saturday 1500-1800	25 %	8.3	7.4	7.7	7.5	7.4	8.9	8.0	7.7	8.1	7.6
	Median	**9.0**	**8.2**	**8.4**	**7.9**	**8.0**	**9.8**	**8.2**	**8.6**	**8.3**	**8.2**
	75 %	10.1	8.5	9.4	8.5	8.5	10.9	8.7	9.1	8.8	8.6
	IQR	**1.8**	**1.1**	**1.7**	**1.0**	**1.1**	**2.0**	**0.7**	**1.4**	**0.7**	**1.0**
	Mean	9.2	8.2	8.7	8.2	8.2	10.1	8.3	8.5	8.6	8.2
	St. Dev.	1.2	1.0	1.3	1.3	1.1	1.4	0.7	1.0	1.1	0.8
	N	24	46	31	45	37	29	33	26	28	35
	t-value		-3.62	-1.33	-2.92	-3.25		-6.23	-4.73	-4.50	-6.78
	P-value		0.001	0.188	0.005	0.002		<0.001	<0.001	<0.001	<0.001
Saturday 1800-2100	25 %	8.7	7.3	7.4	7.6	7.4	8.1	7.2	6.8	7.0	7.0
	Median	**9.1**	**7.6**	**7.9**	**8.0**	**7.9**	**8.6**	**7.8**	**7.5**	**7.5**	**7.6**
	75 %	9.5	8.3	8.3	8.3	8.1	9.2	8.3	8.1	8.1	7.9
	IQR	**0.9**	**1.1**	**0.9**	**0.8**	**0.7**	**1.1**	**1.1**	**1.3**	**1.1**	**0.9**
	Mean	9.1	7.7	8.2	8.1	8.4	9.1	8.0	7.7	7.6	7.6
	St. Dev.	0.6	0.6	1.5	1.2	2.1	1.5	1.3	1.0	0.7	1.3
	N	40	27	33	24	28	18	27	24	38	28
	t-value		-9.06	-3.35	-4.31	-1.87		-2.49	-3.58	-5.11	-3.50
	P-value		<0.001	0.001	<0.001	0.066		0.017	0.001	<0.001	0.001

Table 2. Summary of cost savings for alternative optimization objectives by Section.

Objective		Daily					Annual		
		Total Time Saved (veh-min)	CO_2 Emission Reduction (tons)	CO_2 Savings	User Benefits	Multi-plier	CO_2 Emission Reduction (tons)	CO_2 Savings	User Benefits
(a) System 1, Northern Section									
I	Min Delay	5032	0.71	$16	$1,697	52	37	$810	$88,233
II	Min Delay and Stops	3813	0.54	$12	$1,286	52	28	$614	$66,864
III	Max N_q	1760	0.25	$5	$593	52	13	$283	$30,855
IV	Alt. Max N_q	7883	1.11	$24	$2,658	52	58	$1,268	$138,229
(b) System 2, Southern Section									
I	Min Delay	24386	3.43	$75	$8,223	52	178	$3,924	$427,614
II	Min Delay and Stops	25327	3.56	$78	$8,541	52	185	$4,075	$444,111
III	Max N_q	25147	3.54	$78	$8,480	52	184	$4,046	$440,962
IV	Alt. Max N_q	26338	3.70	$81	$8,882	52	193	$4,238	$461,845
(c) System 1 and System 2, Arterial									
I	Min Delay	29418	4.14	$91	$9,920	52	215	$4,733	$515,847
II	Min Delay and Stops	29140	4.10	$90	$9,826	52	213	$4,689	$510,976
III	Max N_q	26907	3.78	$83	$9,073	52	197	$4,329	$471,817
IV	Alt. Max N_q	34221	4.81	$106	$11,540	52	250	$5,506	$600,073

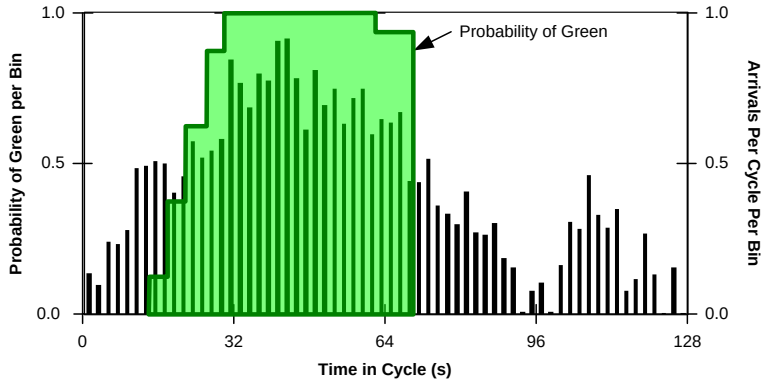

(a) Arrival flow profile and superimposed probability of green.

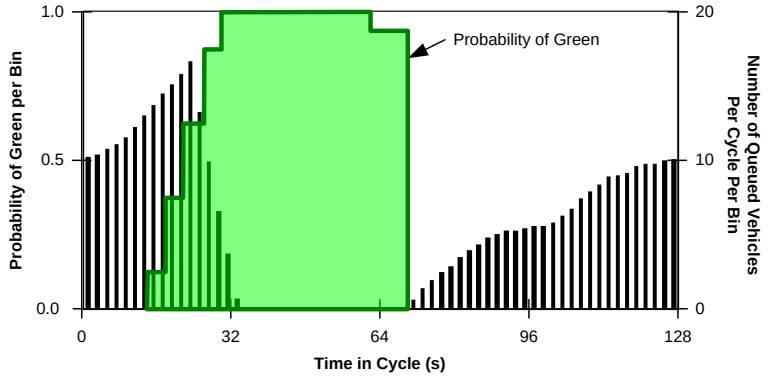

(b) Queue length profile.

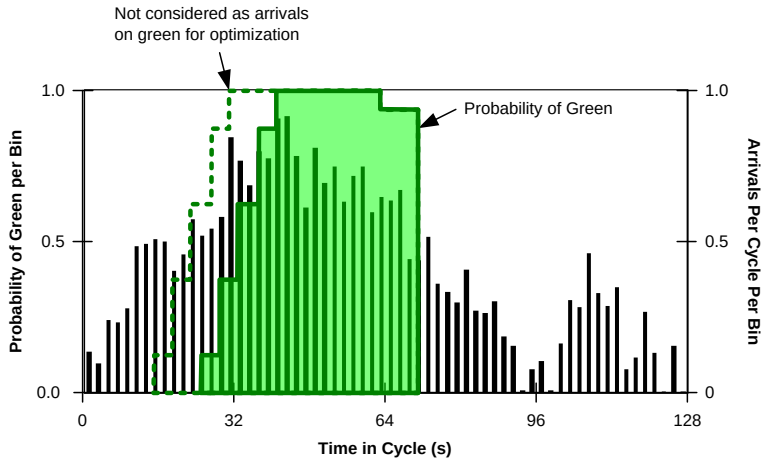

(c) Alternative maximum arrivals on green objective.

Figure 1. Explanation of objective functions using flow profiles.

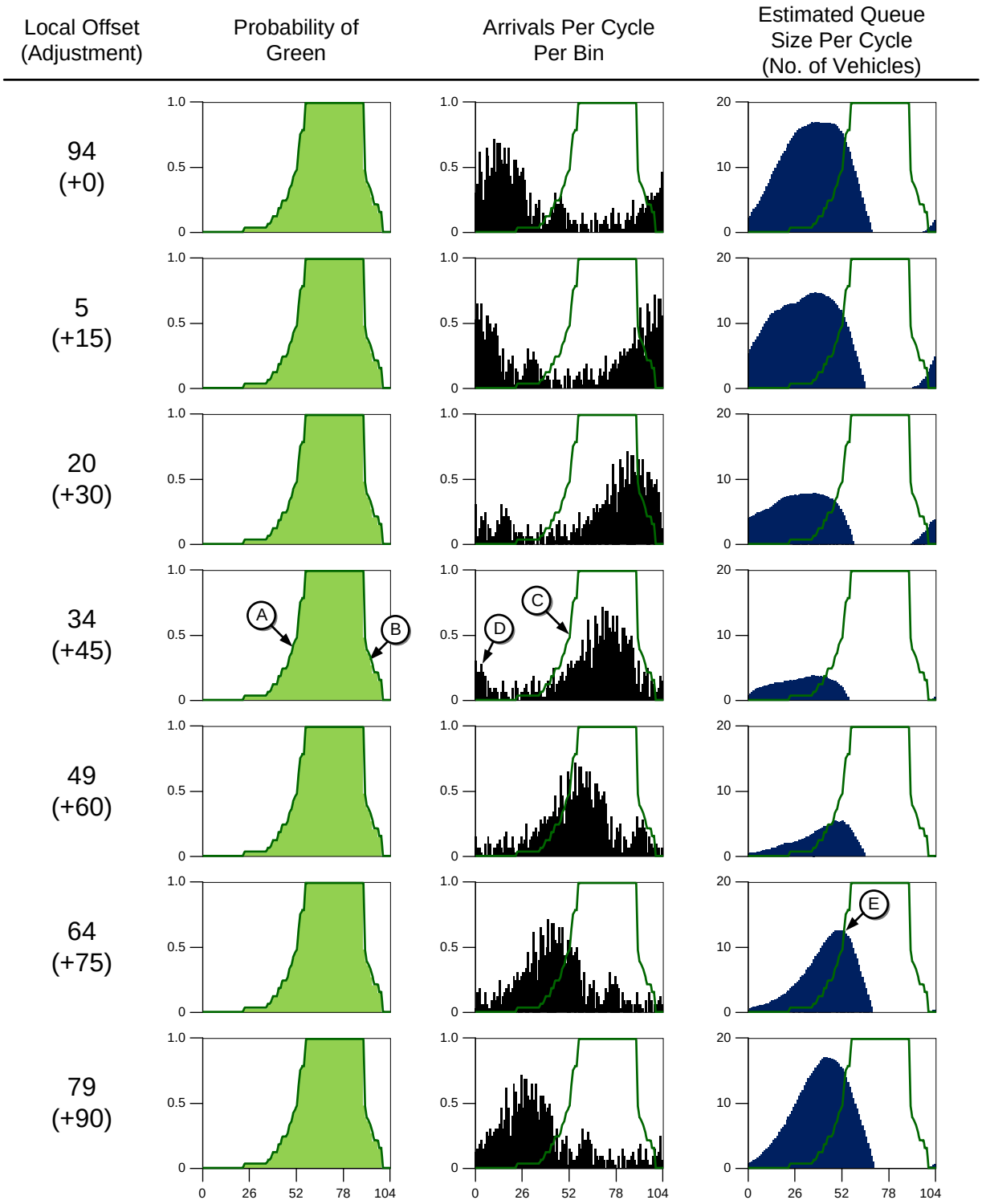

Figure 2. Modeling of alternative adjustments to a local offset on an example coordinated approach (C = 104 s).

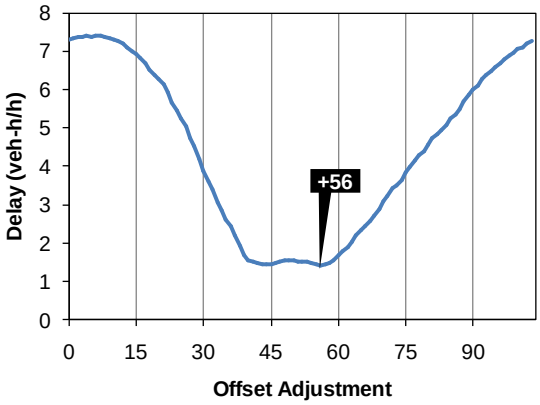

(a) Objective I: Estimated delay.

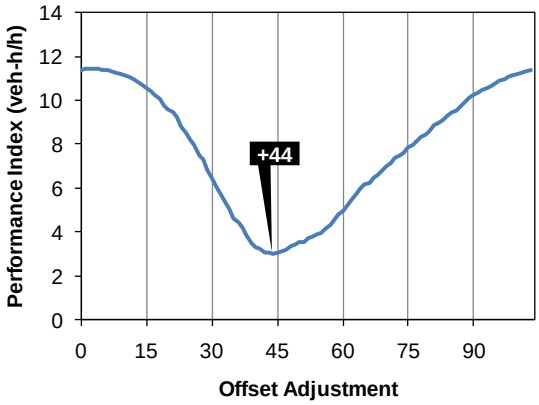

(b) Objective II: Delay and stops.

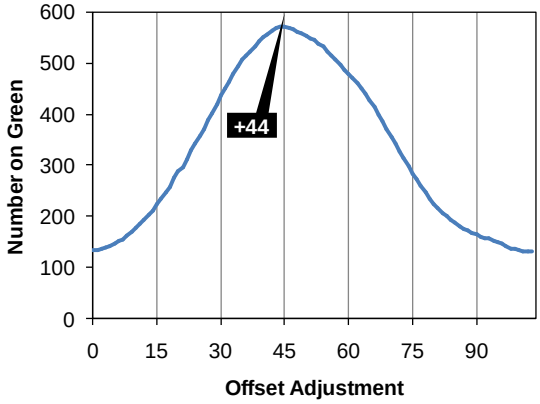

(c) Objective III: Number of arrivals on green.

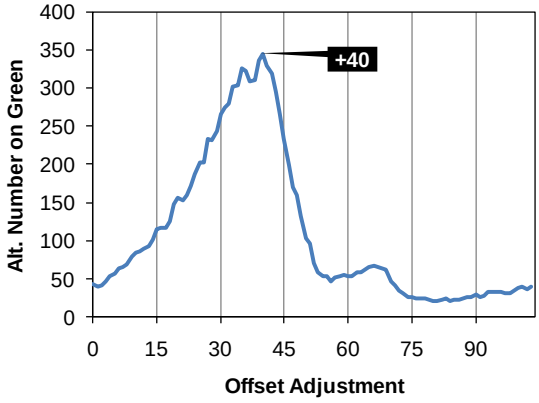

(d) Objective IV: Alternative number of arrivals on green.

Figure 3. Relationship between the four objective functions and offset adjustment on the example coordinated approach (C = 104 s).

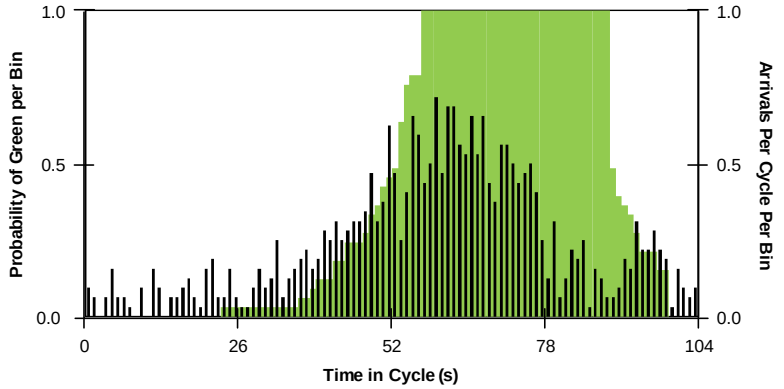

(a) Objective I: Estimated delay (+56).

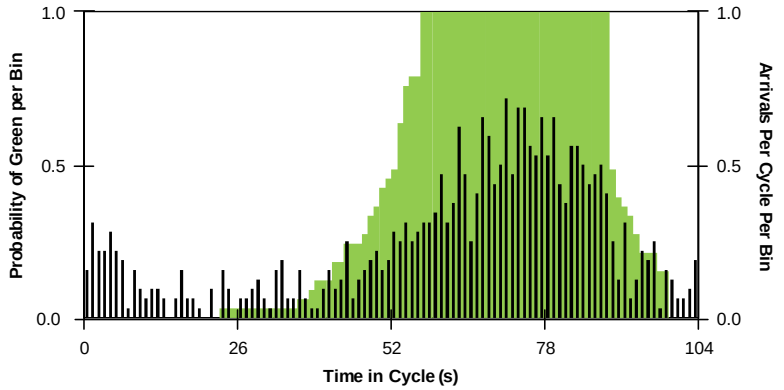

(b) Objective II: Delay and stops and Objective III: Number of arrivals on green (+44).

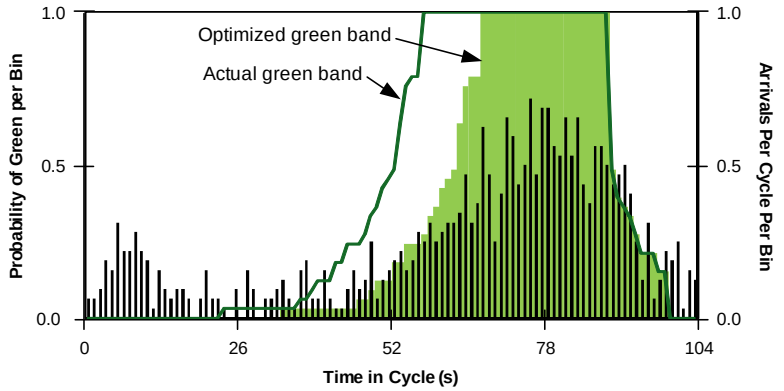

(c) Objective IV: Alternative number of arrivals on green (+40).

Figure 4. Flow profiles for optimal offsets for the example coordinated approach under the four alternative objective functions (C = 104 s).

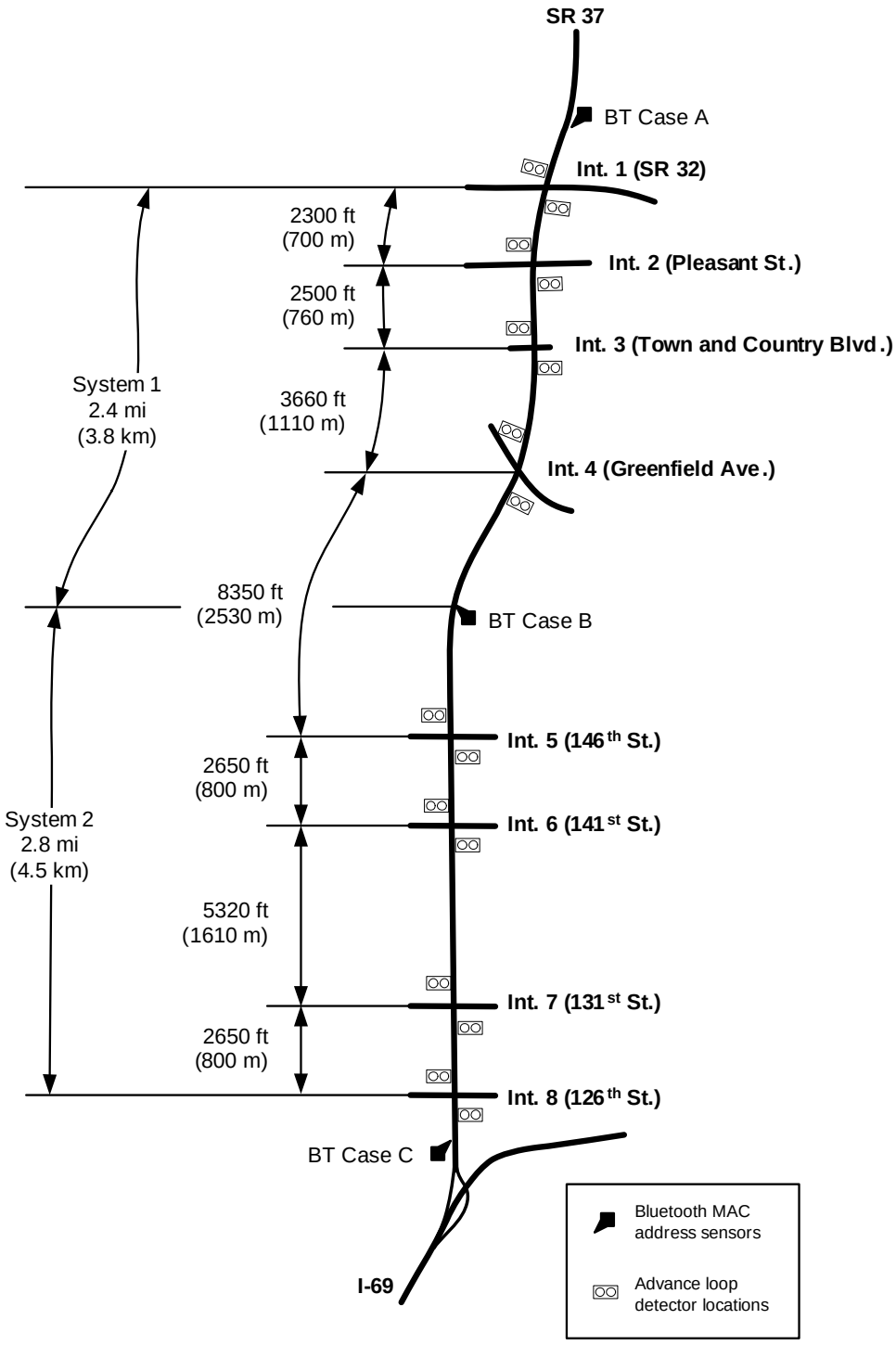

Figure 5. Map of the SR 37 Corridor.

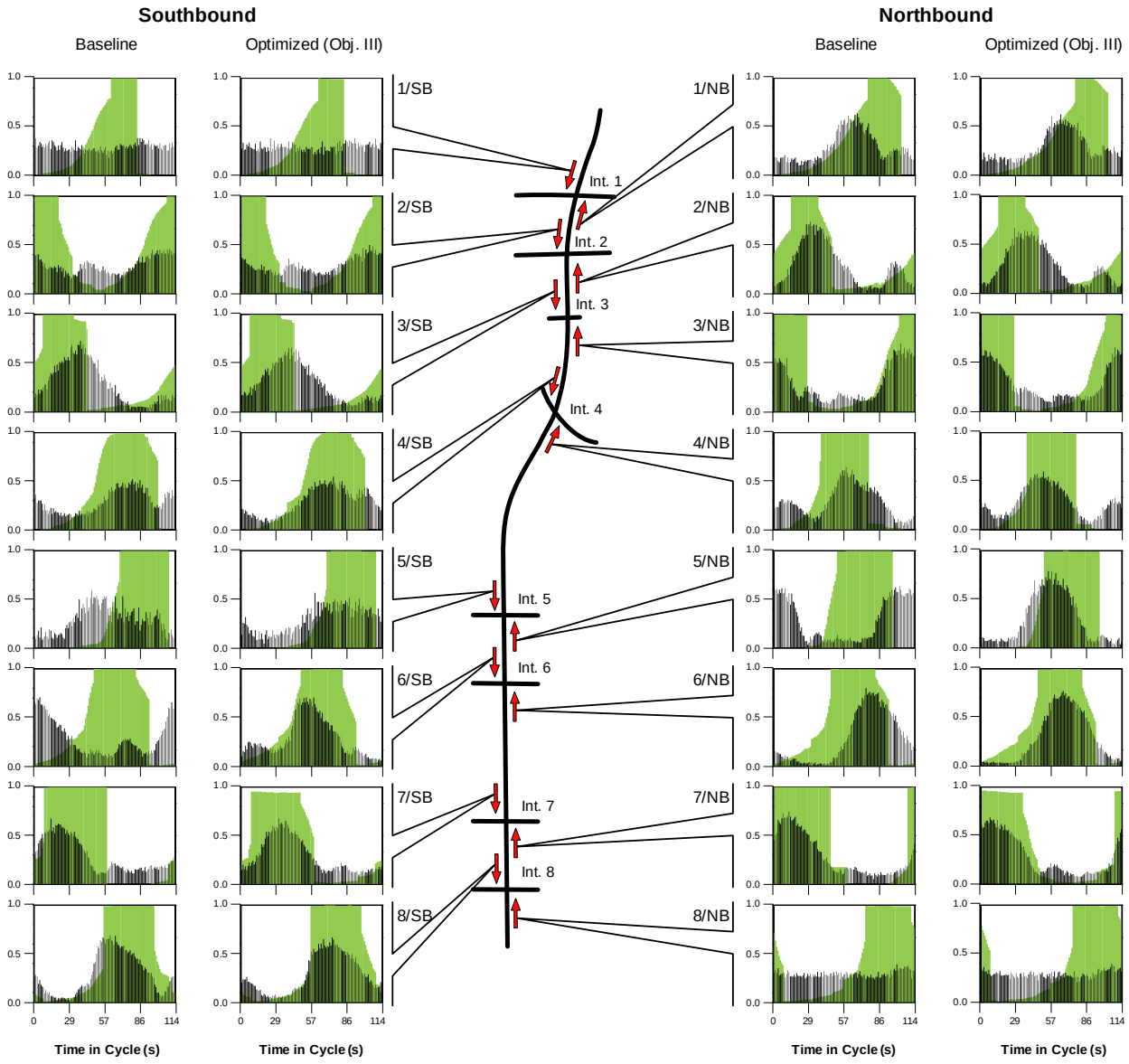

Figure 6. Flow profiles showing flow profiles for baseline and optimized (Objective III) offsets for the Saturday TOD plan.

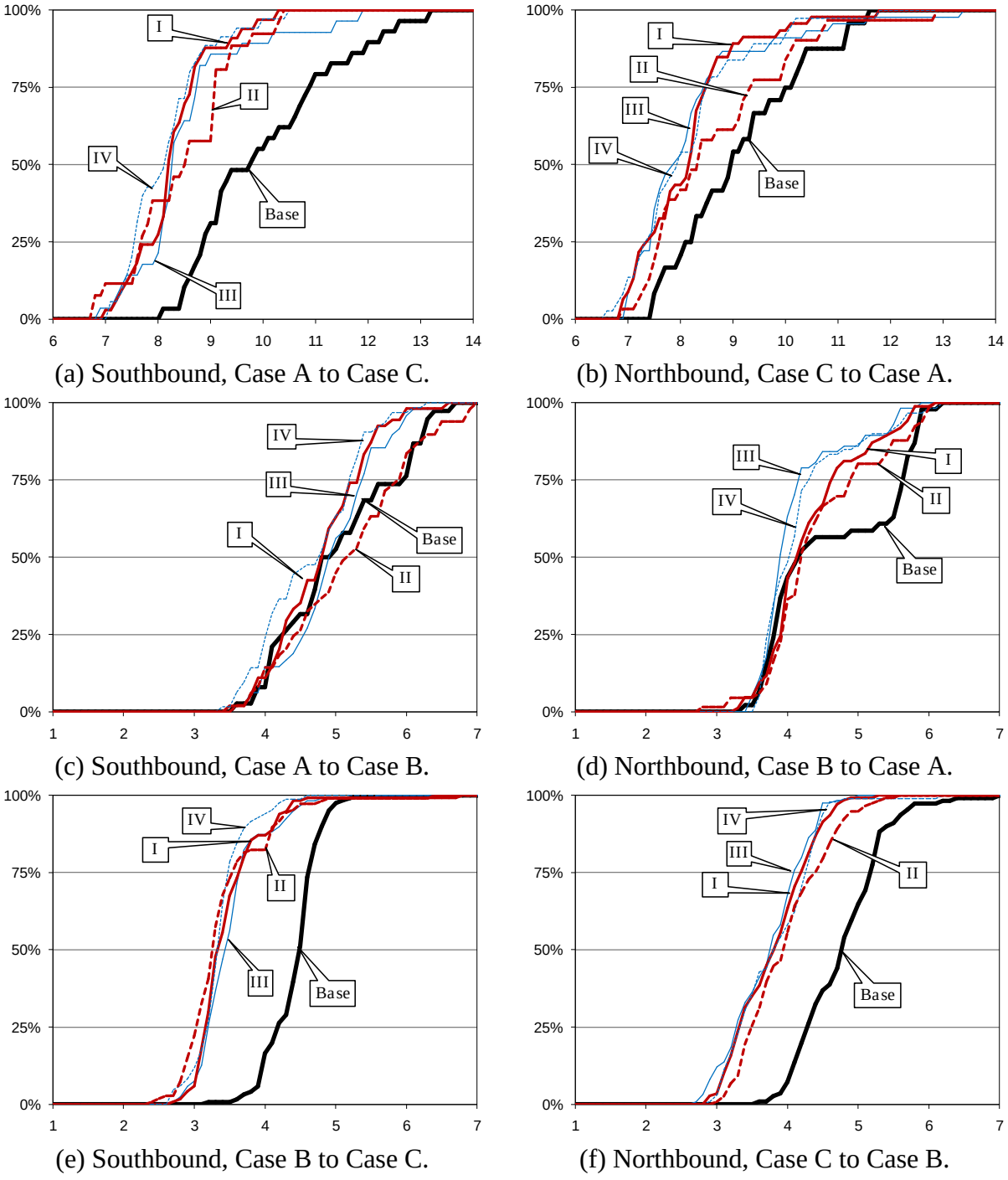

(a) Southbound, Case A to Case C.

(b) Northbound, Case C to Case A.

(c) Southbound, Case A to Case B.

(d) Northbound, Case B to Case A.

(e) Southbound, Case B to Case C.

(f) Northbound, Case C to Case B.

Figure 7. Cumulative frequency diagrams of anonymous probe vehicle travel times for alternative objective functions, Saturday, 1500-1800.

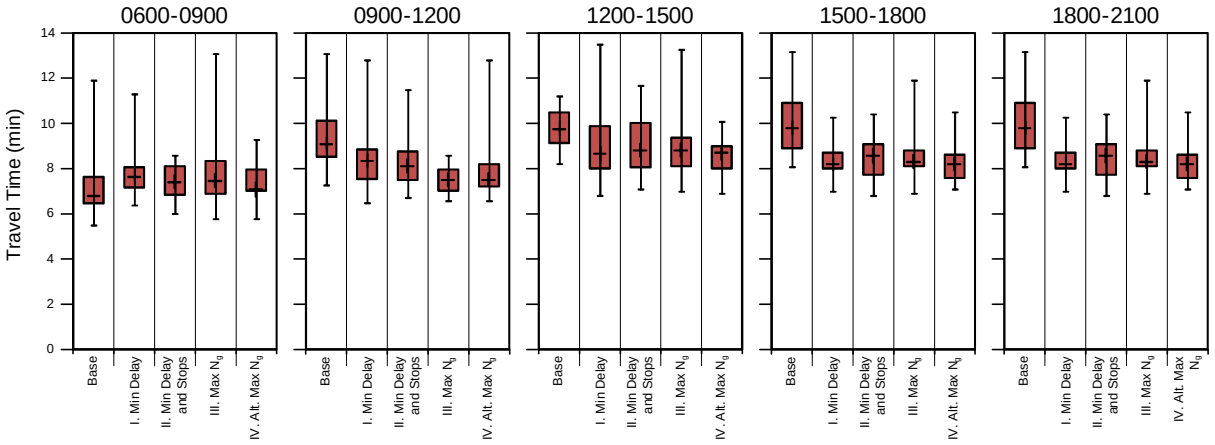

(a) Northbound.

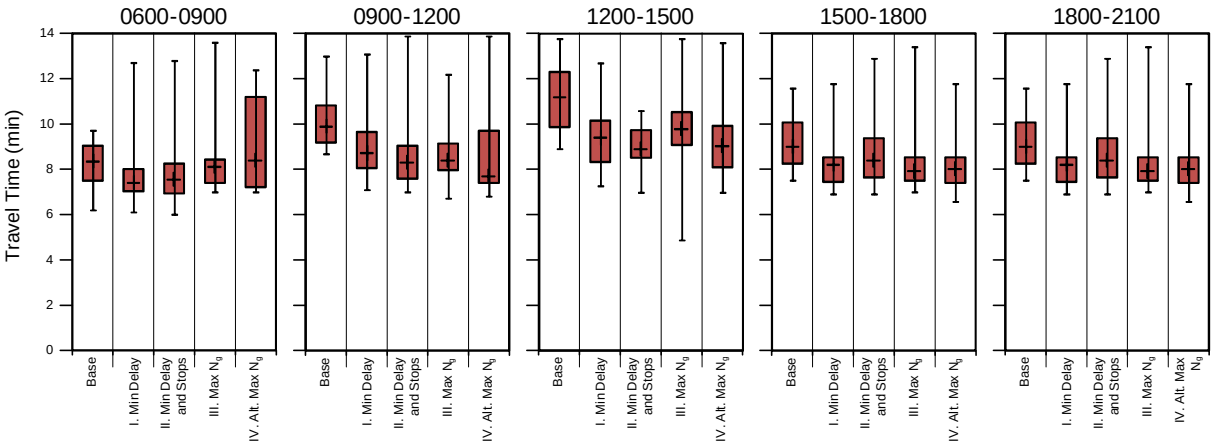

(b) Southbound.

Figure 8. Travel time box-whisker plots for alternative optimization objectives by 3-hour time period, Saturdays, arterial (case A to case C).